Drag reduction in the turbulent Kolmogorov flow

Guido Boffetta,[1] Antonio Celani,[2] and Andrea Mazzino[3]
[1]*Dipartimento di Fisica Generale and INFN, Università degli Studi di Torino, Via Pietro Giuria 1, 10125, Torino, Italy*
[2]*CNRS, INLN, 1361 Route des Lucioles, 06560 Valbonne, France*
[3]*Dipartimento di Fisica and INFN, Università di Genova, Via Dodecaneso 33, 16146 Genova, Italy*
(Received 16 November 2004; published 21 March 2005)

We investigate the phenomenon of drag reduction in a viscoelastic fluid model of dilute polymer solutions. By means of direct numerical simulations of the three-dimensional turbulent Kolmogorov flow we show that drag reduction takes place above a critical Reynolds number Re_c. An explicit expression for the dependence of Re_c on polymer elasticity and diffusivity is derived. The values of the drag coefficient obtained for different fluid parameters collapse onto a universal curve when plotted as a function of the rescaled Reynolds number $\mathrm{Re}/\mathrm{Re}_c$. The analysis of the momentum budget allows us to gain some insight on the physics of drag reduction, and suggests the existence of a Re-independent value of the drag cofficient—lower than the Newtonian one—for large Reynolds numbers.

DOI: 10.1103/PhysRevE.71.036307 PACS number(s): 47.27.−i

I. INTRODUCTION

When a viscous fluid is kept in motion by some external driving, a mean flow is established: the ratio between the work made by the force and the kinetic energy carried by the mean flow is called the *drag coefficient*, or friction factor. This dimensionless number measures the power that has to be supplied to the fluid to maintain a given throughput. When the flow is laminar, the drag coefficient is inversely proportional to the Reynolds number. Upon increasing the intensity of the applied force the flow eventually becomes turbulent, and the drag coefficient becomes approximately independent of the Reynolds number [1], therefore substantially larger than in the viscous case.

In 1949 the British chemist Toms reported that the turbulent drag could be reduced by up to 80% through the addition of minute amounts (few tenths of p.p.m. in weight) of long-chain soluble polymers to water. This observation triggered an enormous experimental activity to characterize this phenomenon (see, e.g., Refs. [2–6]). In spite of these efforts, no fully satisfactory theory of drag reduction is available yet. However, a recent breakthrough has been the observation of drag reduction in numerical simulations of the turbulent channel flow of viscoelastic fluids [7]. Most of the features of experimental flows of dilute polymer solutions are successfully reproduced by these models, even at the quantitative level [8]. Despite these advances, the understanding of drag reduction in the experimentally relevant geometry of pipe or channel flow is still hindered by the complexity of these flows already at the Newtonian level, i.e., in the absence of polymers [9]. This consideration motivated us to investigate simpler geometries in the hope that this may shed some light on the basic physical mechanisms of drag reduction (see, e.g., Ref. [10]).

In this paper we present the results of an extensive numerical investigation of the viscoelastic turbulent Kolmogorov flow. This system has several analogies with the turbulent channel flow, while its main distinctive trait is the absence of material boundaries. Notwithstanding this major difference we will show that drag reduction takes place in the Kolmogorov flow as well. Furthermore, we observe striking quantitative similarities with experimental results in wall-bounded flows: this points to the conclusion that the basic physical mechanisms of drag reduction be substantially independent of the detailed structure of the flow.

II. VISCOELASTIC KOLMOGOROV FLOW

To describe the dynamics of a dilute polymer solution we adopt the linear viscoelastic model (Oldroyd-B) [11]

$$\partial_t \boldsymbol{u} + (\boldsymbol{u}\cdot\nabla)\boldsymbol{u} = -\nabla p + \nu_0 \Delta \boldsymbol{u} + \frac{2\eta\nu_0}{\tau}\nabla\cdot\boldsymbol{\sigma} + \boldsymbol{F}, \quad (1)$$

$$\partial_t \boldsymbol{\sigma} + (\boldsymbol{u}\cdot\nabla)\boldsymbol{\sigma} = (\nabla\boldsymbol{u})^T\cdot\boldsymbol{\sigma} + \boldsymbol{\sigma}\cdot(\nabla\boldsymbol{u}) - 2\frac{\boldsymbol{\sigma}-1}{\tau} + \kappa\Delta\boldsymbol{\sigma}. \quad (2)$$

The velocity field $\boldsymbol{u}$ is incompressible, the symmetric matrix $\boldsymbol{\sigma}$ is the conformation tensor of polymer molecules, and its trace tr $\boldsymbol{\sigma}$ is a measure of their elongation. The parameter τ is the (slowest) polymer relaxation time. The matrix of velocity gradients is defined as $(\nabla\boldsymbol{u})_{ij}=\partial_i u_j$ and $\mathbf{1}$ is the unit tensor. The solvent viscosity is denoted by ν_0 and η is the zero-shear contribution of polymers to the total solution viscosity $\nu = \nu_0(1+\eta)$. The parameter η is proportional to the polymer concentration. The diffusive term $\kappa\Delta\boldsymbol{\sigma}$ is added to prevent numerical instabilities [12]. The constant forcing $\boldsymbol{F} = [F\cos(z/L),0,0]$ maintains the system in a statistically stationary state characterized by a mean flow $\langle\boldsymbol{u}\rangle$. Due to the symmetries of $\boldsymbol{F}$, the only nonzero component of the mean velocity is $\langle u_x\rangle$: it depends on the shear coordinate z alone, vanishes at $z=\pm(\pi/2)L$, and is even under reflections $z\to -z$. Its value at $z=0$, $\langle u_x\rangle_{z=0}$, will be denoted by U. Finally, we establish a short glossary between the Kolmogorov flow and the channel flow: F plays the role of the pressure gradient, πL is analogous to the channel height, and U is equivalent to the centerline velocity.

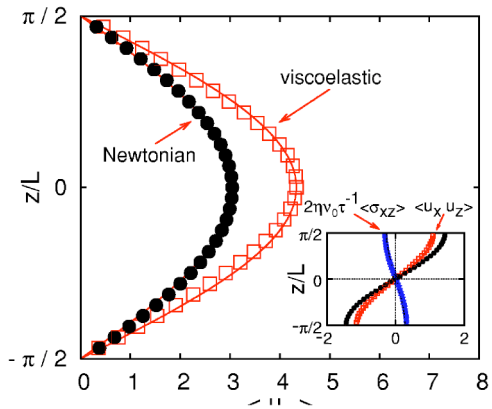

FIG. 1. (Color online) Mean velocity profiles for a Newtonian ($\eta=0$) and a viscoelastic simulation ($\eta=0.3, El=0.019$) at given forcing amplitude $F=1.5$. The measured profiles are undistinguishable from $\langle u_x\rangle = U\cos(z/L)$ (full lines) in both cases. The effect of elasticity is to increase the peak value U with respect to the Newtonian case: in the present case this corresponds to a reduction of the drag coefficient, defined in Eq. (3), of about 40%. In the inset, the profiles of the Reynolds stress $\langle u_x u_z\rangle = S\sin(z/L)$ and the mean polymer stress $2\nu_0\eta\tau^{-1}\langle\sigma_{xz}\rangle = -T\sin(z/L)$. In this case the Reynolds stress is reduced upon polymer addition to approximately 70% of its Newtonian value, consistently with experimental results at comparable drag reduction [14]. The "missing" turbulent shear stress is compensated by the contribution of the polymer stress: the sum of S and T is equal to F in both the Newtonian and viscoelastic case.

III. NUMERICAL EXPERIMENTS

In this framework, we have performed a series of numerical integrations of Eqs. (1) and (2) for a set of values of forcing intensity F, at fixed ν, both for the Newtonian and the viscoelastic case. Comparing results at a given F is equivalent to keeping an imposed pressure gradient—therefore a fixed wall-shear stress—in channel flow experiments (see, e.g., Ref. [13]). Equations (1) and (2) are integrated in a periodic cube of side 2π by means of a fully dealiazed pseudospectral code with 64^3 collocation points. The mean flow length scale is $L=1$ and the viscosity is $\nu = 0.015\,625$. Starting from an initial configuration with a small amount of energy on the smallest modes, after the system evolved into a statistically stationary state, time averages over 100–1000 eddy-turnover times have been performed to obtain the mean profiles of several relevant observables. The latter include the average velocity $\langle u_x\rangle$, the turbulent shear stress (Reynolds stress) $\langle u_x u_z\rangle$, and the mean polymer stress $2\nu_0\eta\tau^{-1}\langle\sigma_{xz}\rangle$.

IV. RESULTS AND DISCUSSION

The mean flow is accurately described by the sinusoidal profile $\langle u_x\rangle = U\cos(z/L)$, both in the Newtonian (see Ref. [15]) and in the viscoelastic flow. However, as shown in Fig. 1, in the viscoelastic case the centerline velocity U is definitely larger: this is the hallmark of drag reduction. It has to be remarked that—at variance with wall-bounded flows where drag reduction is always accompanied by a structural change in the profile (see, e.g., Ref. [3])—in the Kolmogorov flow the increase in throughput takes place just by means of an overall rescaling of the mean velocity. This is due to the different boundary conditions: in channel flows, the profile in the viscous sublayer is left unchanged upon polymer addition while the bulk flow increases substantially. This requires a reshaping of the mean profile, that takes actually place through the increase of the extent of the buffer region (see, e.g., Ref. [13]). In the Kolmogorov flow there is no constraint on velocity profiles, and drag reduction does not necessarily entail their structural change.

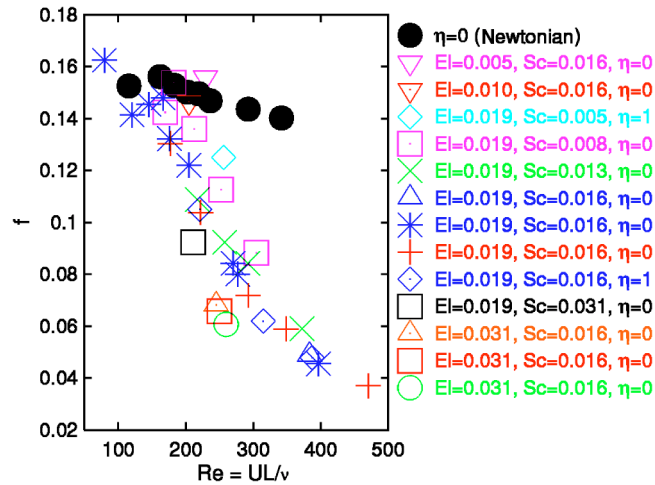

FIG. 2. (Color online) The drag coefficient for different viscoelastic fluid parameters. Data have been collected from numerical simulations at different forcing amplitudes F and viscoelastic parameters η, τ, κ. The statistical error in the determination of f and Re is of the order of the symbols' size.

To quantify the effect of viscoelasticity on the mean flow, we have defined the drag coefficient as

$$f = \frac{FL}{U^2}, \tag{3}$$

and measured its dependence on the Reynolds number $\mathrm{Re} = UL/\nu$. It is natural to use the Reynolds number based on solution viscosity: indeed, for the non-shear-thinning fluid described by Eqs. (1) and (2), ν coincides with the (kinematic) wall viscosity (see, e.g., Refs. [7,8]). It is also possible to define the equivalent of the friction Reynolds number Re_τ, often used in experiments: here, $\mathrm{Re}_\tau = \sqrt{FL^3/\nu^2}$. In the Newtonian case $\mathrm{Re}_\tau \propto \mathrm{Re}$.

For $\mathrm{Re} < \sqrt{2}$ the flow is laminar with mean velocity $U = FL^2/\nu$, giving a drag coefficient $f = \mathrm{Re}^{-1}$. At $\mathrm{Re} \gtrsim 50$ the system is already in a fully developed turbulent state. For a Newtonian fluid, numerical data show that the drag coefficient is approximately independent of Re (see Fig. 2). This behavior agrees with the following classical Kolmogorov argument: since the average energy input $\epsilon = FU/2$ scales as $\epsilon = (\beta/2)U^3/L$ in fully developed turbulence, Eq. (3) yields a constant drag coefficient $f=\beta$. The Newtonian momentum budget gives $F_x = \partial_z\langle u_x u_z\rangle$ (the viscous contribution being

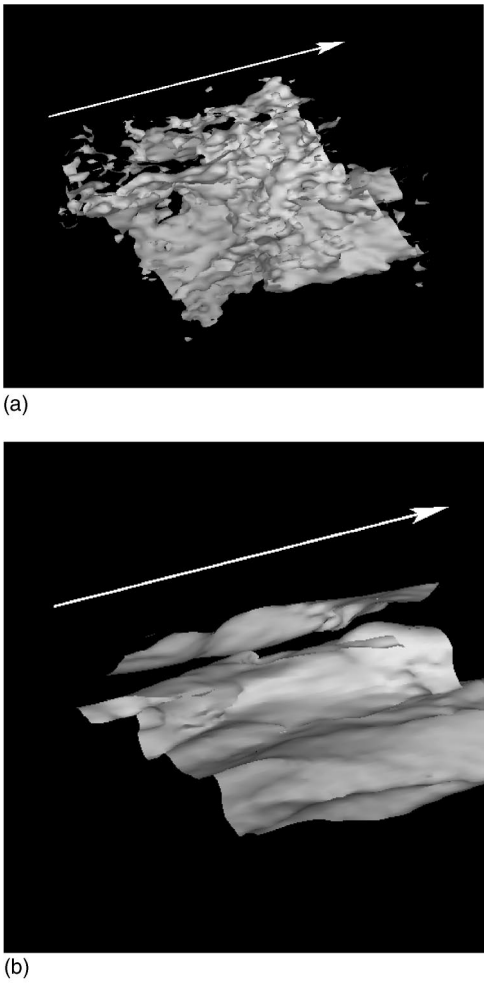

FIG. 3. Snapshots of the isosurfaces $u_x(x,y,z)=U$ for a Newtonian (left) and a viscoelastic simulation (right, $El=0.019$, Sc $=0.016$, $\eta=0.5$). The Reynolds number is Re≈ 350. The arrows show the direction of the mean flow. Small-scale turbulent fluctuations, responsible for kinetic energy dissipation, are suppressed in the viscoelastic case. A high-speed streak in the form of a streamwise oriented tube is visible in the viscoelastic case (right).

negligible) and therefore a Reynolds stress $\langle u_x u_z\rangle = S\sin(z/L)$ with $S=\beta U^2$. For the turbulent Kolmogorov flow, $\beta \simeq 0.15$.

When polymers are added f may be reduced with respect to its Newtonian value, depending on the polymer elasticity $\mathrm{El}=\nu\tau/L^2$, the Schmidt number $\mathrm{Sc}=\nu/\kappa$, and the concentration η, as shown in Fig. 2. For the highest Reynolds number we can attain in our simulations the friction factor is reduced by 75%. Drag reduction is accompanied by changes in the velocity field similar to those occurring in channel flow experiments and simulations: the level of transverse fluctuations $\langle u_z^2\rangle$ is reduced while longitudinal fluctuations $\langle (u_x - \langle u_x\rangle)^2\rangle$ increase and high streamwise velocity streaks are observed (see Fig. 3). Incidentally, we notice that drag reduction is observed at Reynolds numbers definitely smaller than the typical experimental values: this is possible thanks to the relatively high value of elasticity utilized in our simulations. Comparable parameters have been used in numerical simulations of the channel flow as well (see, e.g., Ref. [7]), and produced a similar effect on the threshold for drag reduction.

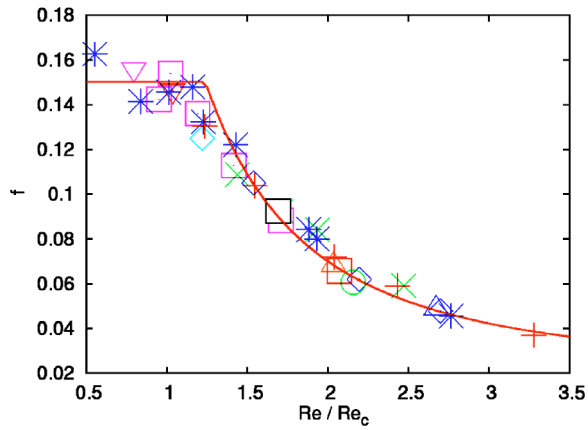

FIG. 4. (Color online) The drag coefficient plotted as a function of the rescaled Reynolds number $\mathrm{Re}/\mathrm{Re}_c$. Symbols as in Fig. 2. The full line is Eq. (5) with $\beta=0.15$, $\gamma=0.2$, and $\delta=0.02$.

From the inspection of Fig. 2 we notice some systematic trend: at moderate Reynolds numbers (Re$\lesssim 200$) viscoelastic effects do not alter substantially the value of the drag coefficient; at larger Re polymers with a higher elasticity are more effective as drag-reducing agents; conversely, polymers with higher diffusivity are less effective. To understand the variation of the drag coefficient with fluid parameters, we sought a dependence of the form $f=\varphi(\mathrm{Re}/\mathrm{Re}_c)$ where $\mathrm{Re}_c(\mathrm{El},\mathrm{Sc},\eta)$ is the critical Reynolds number for the onset of drag reduction. To obtain an explicit expression for Re_c we need to extend the argument given by Ref. [16] to the case of finite polymer diffusivity. The reasoning goes as follows: for polymers to be substantially elongated, stretching must prevail over elastic relaxation and diffusivity. This argument is just a revised version of the Lumley's (1969) "time criterion." Accordingly, at the onset, the terms appearing in Eq. (2) must then satisfy $(\nabla u)_c \sim 2/\tau + \kappa/L^2$; since the transition is incipient we can estimate the typical velocity gradient as $(\epsilon_c/\nu)^{1/2}$, and utilizing the expression $\epsilon_c \propto U_c^3/L$ we finally obtain

$$\mathrm{Re}_c \propto \left(\frac{2}{\mathrm{El}} + \frac{1}{\mathrm{Sc}}\right)^{2/3}. \tag{4}$$

For vanishing diffusivity we recover the result by Ref. [16].

In Fig. 4 we present the same data as in Fig. 2, now plotted against the rescaled Reynolds number $\mathrm{Re}/\mathrm{Re}_c$. The good quality of the collapse supports the validity of the relation $f=\varphi(\mathrm{Re}/\mathrm{Re}_c)$. The function φ is universal with respect to the choice of fluid parameters. Its shape will be derived in the following, with the aid of simple assumptions, starting from the equation for momentum conservation (see Ref. [17] for a similar approach to wall-bounded flows).

Upon time averaging, Eq. (1) reduces to $F_x = -\nu_0 \partial_z^2 \langle u_x\rangle + \partial_z(\langle u_x u_z\rangle - 2\nu_0\eta\langle\sigma_{xz}\rangle/\tau)$. Utilizing the numerical observation that the Reynolds stress $\mathcal{S}=\langle u_x u_z\rangle = S\sin(z/L)$ and the

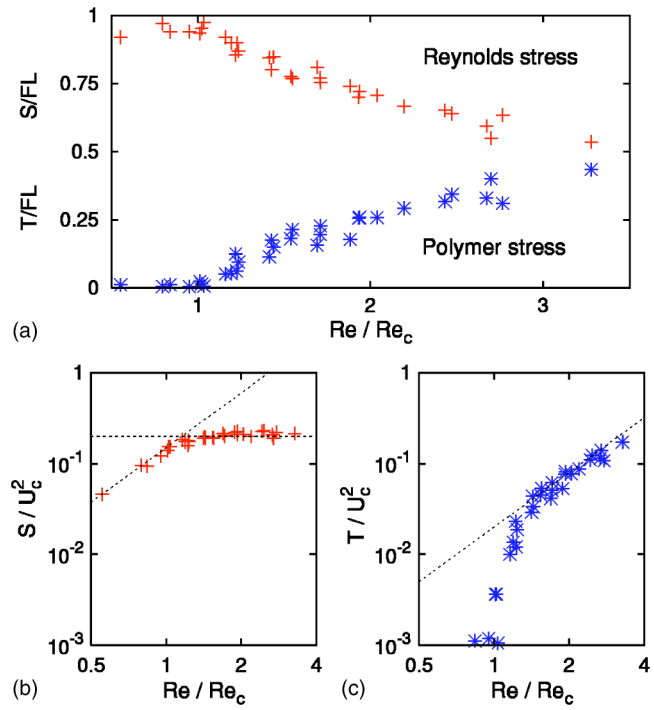

FIG. 5. (Color online) (a): Peak values of the Reynolds stress $\langle u_x u_z \rangle = S \sin(z/L)$, and of the polymer stress $2\eta\nu_0\tau^{-1}\langle\sigma_{xz}\rangle = -T \sin(z/L)$, nondimensionalized by the total stress FL. The sum $(S+T)/(FL)$ nearly equals unity for each couple of data points, confirming that the viscous (solvent) stress $\nu_0 U/L^2$ is negligible at the present Reynolds numbers. (b) The Reynolds stress S and (c) the polymer stress T nondimensionalized by the squared critical velocity U_c^2: The full lines are $S/U_c^2 = \gamma$ (left, horizontal), $S/U_c^2 = \beta(\mathrm{Re}/\mathrm{Re}_c)^2$ (left, oblique), $T/U_c^2 = \delta(\mathrm{Re}/\mathrm{Re}_c)^2$ (right). The numerical parameters are $\beta = 0.15$, $\gamma = 0.2$, and $\delta = 0.02$.

polymer stress $\mathcal{T} = 2\nu_0\eta\langle\sigma_{xz}\rangle/\tau = -T \sin(z/L)$, we obtain the momentum budget $F = \nu_0 U/L^2 + S/L + T/L$. The contribution $\nu_0 U/L^2$ is relevant only in the laminar regime, and can therefore be neglected. The dependence of the stresses on the rescaled Reynolds number is presented in Fig. 5. Below the threshold the polymer stress is vanishingly small whereas the Reynolds stress is $S \simeq \beta U^2 \simeq FL$ in agreement with the observation of a Re-independent drag coefficient. Above Re_c, the polymer stress makes a significant contribution to the momentum budget. At the largest Re we can attain, the elastic stress reaches almost 50% of the total stress, not far from experimental results by Ref. [18]. Rescaling the stresses with the critical velocity squared shows that above the onset S tends to a constant value γU_c^2 [see Fig. 5(b)], and the polymer stress follows the law $T = \delta U^2$ [Fig. 5(c)]. The physical interpretation of these observations is that above the onset of drag reduction an increasing fraction of the momentum injected by the external force is sequestered by polymers, which are, however, less effective in absorbing it than transverse velocity fluctuations ($\delta < \beta$). This results in an enhancement of the mean flow with respect to the Newtonian case, i.e., drag reduction. Inserting the empirical expressions for S and T, the momentum budget above the onset reads $F = \gamma U_c^2/L + \delta U^2/L$, and the resulting drag coefficient is

$$f = \begin{cases} \beta & \text{for } \mathrm{Re} \lesssim \mathrm{Re}_c, \\ \gamma\left(\dfrac{\mathrm{Re}_c}{\mathrm{Re}}\right)^2 + \delta & \text{for } \mathrm{Re} \gtrsim \mathrm{Re}_c. \end{cases} \tag{5}$$

This expression is compared with numerical results in Fig. 4, where the values of the parameters γ and δ have been obtained from the data shown in Fig. 5. The agreement is excellent, except possibly for $\mathrm{Re} \approx \mathrm{Re}_c$, where Eq. (5) predicts an abrupt transition: from Fig. 5 this rather appears to be a smooth crossover, whose actual shape cannot be extracted by means of simple arguments. The actual values of β, γ, and δ are not of utmost importance since they are likely to depend on the details of the driving force, and therefore on the shape of the velocity profile. What is crucial to drag reduction is that $\delta < \beta$, or—in plain words—that momentum is transferred with greater ease to velocity fluctuations than to elastic ones. Understanding the reasons for this difference would disclose the basic physical mechanisms of drag reduction.

Remarkably, Eq. (5) suggests the existence of a minimal value for the drag coefficient in the limit of large Re. In this ultimate regime momentum transfer would take place only through polymer stresses. However, the present data do not cover a sufficient span of values of Re to allow us to confirm or reject this prediction.

We end up by addressing the issue of the role of polymer concentration in the determination of the critical Reynolds number. The results shown in Fig. 4 do show a very weak dependence on η, compatible with the value $\mathrm{Re}_c \propto (1+\eta)^{-2/3}$ than can be obtained from Eq. (4). This result is at variance with experimental findings in pipe and channel flows, where Re_c is a clearly decreasing function of the concentration. We argue that this discrepancy is due to the linear character of the viscoelastic model adopted here. Indeed, following Ref. [19], let us repeat the argument that leads to Eq. (4), now for a nonlinear elastic model (e.g., FENE-P) with a stress-dependent relaxation time $\tau/g(\mathrm{tr}\,\boldsymbol{\sigma})$, where g is an increasing function of polymer elongation and equals unity in the linear range. The time criterion in this case yields $\mathrm{Re}_c = \mathrm{El}^{2/3}[g(\mathrm{tr}\,\boldsymbol{\sigma})]^{2/3}$ (the dependence on diffusivity is omitted for sake of simplicity). At small concentrations the typical polymer extension will be very large, since the feedback on the velocity field is proportional to η. At larger concentrations, smaller values of $\mathrm{tr}\,\boldsymbol{\sigma}$ suffice to maintain the system in a stationary state. In the linear phase, we have that $\mathrm{tr}\,\boldsymbol{\sigma} \propto \eta^{-1}$ for extended polymers. We expect that the typical polymer extension would be a decreasing function of η, and therefore Re_c an increasing function of concentration for nonlinear models. The numerical verification of this expectation lies beyond the scope of the present paper and will be addressed in the near future.

To summarize, we have investigated the problem of turbulent drag reduction by polymer additives in the context of

linear viscoelastic fluid models. For the turbulent Kolmogorov flow we have shown that the drag coefficient can be expressed as a function of the rescaled Reynolds number only, that this function is universal with respect to the fluid characteristics, and that its shape can be derived by simple phenomenological arguments. The analysis of the effect of polymer diffusivity as well as the investigation of concentration dependence in nonlinear models will be the subject of future work. Numerical simulations at higher resolution should allow to settle these issues.

ACKNOWLEDGMENTS

We thank R. Benzi, M. Chertkov, B. Eckhardt, I. Procaccia, V. Steinberg, and M. Vergassola for valuable discussions. We acknowledge the support of EU under Contract No. HPRN-CT-2002-00300 "Stirring and Mixing" and of MIUR-Cofin 2003 "Sistemi Complessi e Problemi a Molti Corpi." Numerical simulations have been performed at CINECA (INFM parallel computing initiative).

[1] O. Reynolds, Philos. Trans. R. Soc. London **174**, 935 (1883).
[2] J. Lumley, Annu. Rev. Fluid Mech. **1**, 367 (1969).
[3] P. S. Virk, AIChE J. **21**, 625 (1975).
[4] W. D. D. Mc Comb, *The Physics of Fluid Turbulence* (Oxford University Press, New York, 1992).
[5] R. H. Nadolink and W. W. Haigh, Appl. Mech. Rev. **48**, 351 (1995).
[6] K. R. Sreenivasan and C. M. White, J. Fluid Mech. **409**, 149 (2000).
[7] R. Sureshkumar *et al.*, Phys. Fluids **9**, 743 (1997).
[8] P. K. Ptasinski *et al.*, J. Fluid Mech. **490**, 251 (2003).
[9] E. De Angelis *et al.*, Phys. Rev. E **67**, 056312 (2003).
[10] E. De Angelis *et al.*, nlin.CD/0208016.
[11] R. B. Bird *et al.*, *Dynamics of Polymeric Fluids* (Wiley, New York, 1987), Vol. 2.
[12] R. Sureshkumar and A. N. Beris, J. Non-Newtonian Fluid Mech. **60**, 53 (1995).
[13] T. S. Luchik, and W. G. Tiederman, J. Fluid Mech. **190**, 241 (1988).
[14] W. W. Willmarth *et al.*, Phys. Fluids **30**, 933 (1987).
[15] Sinusoidal mean profiles were observed in Newtonian ($\eta=0$) turbulence by V. Borue and S. A. Orszag, J. Fluid Mech. **306**, 293 (1996). See also the related work by J. V. Shebalin and S. L. Woodruff, Phys. Fluids **9**, 164 (1997).
[16] E. Balkovsky *et al.*, Phys. Rev. E **64**, 056301 (2001).
[17] V. S. L'vov *et al.*, Phys. Rev. Lett. **92**, 244503 (2004).
[18] P. K. Ptasinski *et al.*, Flow, Turbul. Combust. **66**, 159 (2001).
[19] R. Benzi, E. S. C. Ching, N. Horesh, and I. Procaccia, Phys. Rev. Lett. **92**, 078302 (2004).